Formation of nano-dispersed Cu particles during aging of a Fe-Cu alloy and dislocation effect

Lili Zhang, Hongxiang Jiang, Jiuzhou Zhao*

Institute of Metal Research, Chinese Academy of Sciences, 72 Wenhua Road, Shenyang 110016, China

*Corresponding author: Tel: (+86) 24 23971918; E-mail: jzzhao@imr.ac.cn

DOI: 10.5185/amlett.2019.2119
www.vbripress.com/aml

Abstract

The microstructure evolution in a Fe-Cu alloy with/without pre-deformation during the aging treatment is investigated numerically. The results demonstrate that although the Cu precipitates first nucleate on dislocations, the summit of the nucleation rate occurs in the matrix. Most of Cu particles situate in the matrix immediately after the nucleation. The preferential dissolution of Cu precipitates in the matrix occurs during the Ostwald repining stage, and the vast majority of the residual particles situate on dislocations in an overaged alloy. Copyright © 2019 VBRI Press.

Keywords: Fe-Cu alloy, aging, dislocation, precipitation, modeling.

Introduction

Dispersed nano Cu particles may form during the aging treatment of a Fe-Cu alloy or steel containing Cu. The microstructure evolution during aging is very complicated. It may involve nucleation, growth/shrinkage and structural transformation of the precipitates. A lot of work has been done to investigate the age hardening characteristics of the predeformed Cu bearing steels [**1-4**]. However, up to date, the exact role of dislocations during the precipitation process is still under dispute. This work is carried out to clarify the dislocation effect on the microstructure formation during aging a Fe-Cu alloy.

Formulas

When a Fe-Cu alloy is aged, Cu particles with a structure of metastable body-centered cubic (bcc) first nucleate and grow/coarsen. When reaching a critical size, these particles then transform to a structure of face-centered cubic (fcc) with high density of twins (9R). The twins finally disappear and the precipitates show a equilibrium fcc structure. Researches demonstrate that the Cu particles with a diameter of 17 nm still remain 9R structure. Particles with the equilibrium fcc structure are observed only after aging for a time longer than 100 h [**5**]. The 9R→fcc structural transformation is thus omitted in this study. Let $f^{\mathrm{i}}dR$ (i = bcc or 9R) is the number of the bcc (i = bcc) or 9R (i = 9R) precipitates per unit volume in a radius range $R \sim R+dR$ at time t. During aging, f^{i} satisfies:

$$\frac{\partial f^{\mathrm{i}}}{\partial t}+\frac{\partial}{\partial R}\left(v^{\mathrm{i}} f^{\mathrm{i}}\right)=\left.\frac{\partial I^{\mathrm{i}}}{\partial R}\right|_{R=R^*} \tag{1}$$

where v^{i} and I^{i} are respctively the growth/shrinkage rate and nucleation rate of the precipitates with bcc (i = bcc) or 9R (i = 9R) structure. R^* is the critical nucleus radius.

With the aging time going on, the content of the precipitates and the concentration of the matrix may vary. However, the initial solute Cu concentration C^0 is conserved at all times:

$$C^0=(1-\varphi)C^{\mathrm{m}}+\sum\left(\varphi^{\mathrm{i}}C^{\mathrm{i}}\right) \tag{2}$$

where $\varphi=\sum\varphi^{\mathrm{i}}$ is the volume fraction of the precipates, φ^{i} and C^{i} are respectively the volume fraction and the concentration of the precipitates with a structure of bcc (i = bcc) or 9R (i = 9R), C^{m} is the solute Cu concentration of the matrix.

The nucleation rate I^{j} (j = m or dis) of the precipitates in the matrix (j = m) or along the dislocation (j = dis) can be calculated by:

$$I^{\mathrm{j}}=Z^{\mathrm{j}}\beta^{\mathrm{j}}N_{\mathrm{v}}^{\mathrm{j}}\exp\left(-\frac{\Delta G_{\mathrm{c}}^{\mathrm{j}}}{k_{\mathrm{B}}T}\right)\exp\left(-\frac{\tau^{\mathrm{j}}}{t}\right) \tag{3}$$

where $Z^{\mathrm{j}}=\dfrac{v_{\alpha}\left(\Delta G_{\mathrm{v}}\right)^2}{8\pi\left[k_{\mathrm{B}}T\left(\sigma^{\mathrm{bcc/j}}\right)^3\right]^{1/2}}$ is the Zeldovich factor, v_{α} is the atomic volume in the nucleus, k_{B} is the Boltzmann's constant, T the thermodynamic temperature, $\sigma^{\mathrm{bcc/j}}$ the precipitate/matrix (j = m) or precipitate/dislocation (j = dis) interfacial energy, ΔG_{v} the gain in free energy per volume on precipitation [**6**].

$\beta^{\mathrm{j}}=\frac{S^{*}D^{\mathrm{j}}C_{\mathrm{m}}}{a^{4}}$ is the attachment rate of atoms to a critical nucleus, S^{*} is the surface area of a critical nucleus, D^{j} is the diffusion coefficient of Cu in the matrix (j=m) or along the dislocation (j=dis), a is the lattice parameter. $N_{\mathrm{v}}^{\mathrm{j}}$ is the number density of atoms in the matrix (j=m) or on dislocations (j=dis). $\Delta G_{\mathrm{c}}^{\mathrm{j}}=\frac{16\pi\left(\sigma^{\mathrm{bcc/j}}\right)^{3}}{3\left(\Delta G_{\mathrm{v}}\right)^{2}}$ is the energy barrier for the formation of a critical nucleus. $\tau^{\mathrm{j}}=\frac{8k_{\mathrm{B}}T\sigma^{\mathrm{bcc/j}}a^{4}}{v_{\alpha}^{2}\left(\Delta G_{\mathrm{v}}\right)^{2}D^{\mathrm{j}}C^{\mathrm{m}}}$ is the incubation time.

The interfacial energies $\sigma^{\mathrm{bcc/m}}$ and $\sigma^{\mathrm{bcc/dis}}$ are respectively calculated by using Eqs. (4a) [**7, 8**] and (4b) [9]:

$$\sigma^{\mathrm{bcc/m}}=1.08\frac{k_{\mathrm{B}}}{a^{2}}\left(T_{\mathrm{c}}^{'}-T\right) \tag{4a}$$

$$\sigma^{\mathrm{bcc/dis}}=\sigma^{\mathrm{bcc/m}}-\frac{\mu\boldsymbol{b}\left|\varepsilon\right|(1+\upsilon)}{9\pi(1-\upsilon)} \tag{4b}$$

where $T_{\mathrm{c}}^{'}=\frac{\Omega-TS^{\mathrm{nc}}}{2k_{\mathrm{B}}}$ with Ω and S^{nc} respectively being the segregation energy and the non-configurational entropy, a value of 6800 K is used for $\frac{\Omega}{k_{\mathrm{B}}}$ and 3 for $\frac{S^{\mathrm{nc}}}{k_{\mathrm{B}}}$ [8]. μ , $\boldsymbol{b}$, ε and υ are respectively the shear modulus, Brugers vector of the dislocation, misfit strain of the particle in the matrix and Poisson's ratio [**9**].

The Cu diffusion coefficient in the matrix and along dislocations can be respectively calculated by [**4, 10**]:

$$D^{\mathrm{m}}=D_{0}\exp\left(-\frac{E}{k_{\mathrm{B}}T}\right) \tag{5a}$$

$$D^{\mathrm{dis}}=(4D_{\mathrm{P}}D_{\mathrm{Fe}}^{2})^{1/3} \tag{5b}$$

where E=2.29 ev is the diffusion activation energy of Cu atoms in iron [**11**], D_{0} is a constant and can be obtained through the Cu diffusion coefficient at 773 K, which is $7.7\times10^{-19}\,\mathrm{m^{2}s^{-1}}$ [**12**]. D_{P} is the pipe diffusion coefficient along dislocations [**13, 14**] and D_{Fe} the self-diffusion coefficient of bcc Fe.

The growth rate v^{i} of the bcc (i=bcc) or 9R (i=9R) particles is calculated by [**15**]:

$$v^{\mathrm{i}}=D^{\mathrm{j}}\left[1+R(\langle R\rangle\varphi N)^{1/2}\right]\frac{C^{\mathrm{m}}-C_{\mathrm{I}}^{\mathrm{i}}}{C^{\mathrm{i}}-C_{\mathrm{I}}^{\mathrm{i}}}\frac{1}{R} \tag{6}$$

where $\langle R\rangle$ and N are respectively the average radius and the number density of the Cu particles, $C_{\mathrm{I}}^{\mathrm{i}}=C_{\mathrm{me}}^{\mathrm{i}}\exp\left(\frac{\alpha_{\mathrm{S}}}{R}\right)$ is the solute Cu concentration in the matrix at the inter-phase boundary with α_{S} being the capillary length, $C_{\mathrm{me}}^{\mathrm{i}}$ is the solute Cu concentration in the matrix at the flat interface of matrix/bcc precipitates (i=bcc) or matrix/9R precipitates (i=9R), which can be calculated by [**4, 7, 12**]:

$$C_{\mathrm{me}}^{\mathrm{bcc}}=\exp\left(-\frac{2T_{\mathrm{c}}'}{T}\right) \tag{7a}$$

$$C_{\mathrm{me}}^{\mathrm{9R}}=\frac{C_{\mathrm{me}}^{\mathrm{bcc}}}{1.5} \tag{7b}$$

According to the experimental results [**5, 16**], the critical radius for the 9R→fcc transformation can be estimated as 2.2 nm.

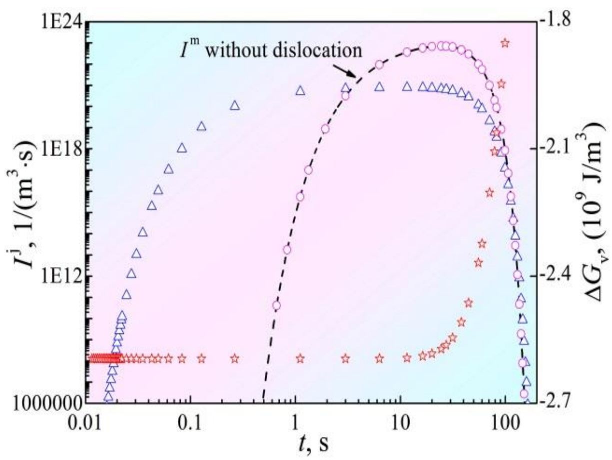

Fig. 1. Nucleation rate of Cu particles in the matrix (circles) and on dislocations (triangles) and driving force (stars) for the precipitation by assuming that the initial dislocation density is 8.8×10^{13} m^{-2} and the heating rate from 298 to 773 K is 10^{6} K/s. The dashed line is the nucleation rate of Cu particles calculated for the specimen without dislocations.

Numerical results and discussion

The above equations are solved numerically for Fe-1.3 at% Cu alloy using finite volume method [**17, 18**]. The dislocation density of the alloy with a 10% deformation is 8.8×10^{13} m^{-2} and it drops to 10^{13} m^{-2} after the alloy is aged at 773 K for 20 min [3]. It is assumed in the calculations that the annihilation rate is direct proportion to the dislocation density and the Cu particles nucleate competitively on dislocations and in the matrix. **Fig. 1** and **Fig. 2** show the ΔG_{v} and I^{j}, N and $\langle R\rangle$. The results demonstrate that Cu particles first nucleates on dislocations **(**see **Fig. 1)** due to the fact that dislocations can reduce $\Delta G_{\mathrm{c}}^{\mathrm{dis}}$, enhance D^{j} and thus lead to an increase in β^{dis} and a decrease in τ^{dis}. Thereafter, the microstructure evolution is determined by the combined effect of the nucleation and diffusional growth of Cu particles. During the early period of nucleation, there is no precipitation in the matrix and ΔG_{v} almost keeps constant (see **Figs. 1** and **2**). Then the precipitates begin to nucleate in the matrix and N increases steeply. The appearance of dislocations does not affect I^{m}. The maximum I^{m} is several orders of magnitude greater than I^{dis} (see **Fig. 1**). The vast majority of the Cu particles thus locate in the matrix immediately after nucleation (see **Fig. 2**). ΔG_{v} decreases quickly due to the nucleation and growth of the precipitates (see **Fig. 1**). The coarsening process of precipitates begins soon and N decreases steeply. The Cu particles in the matrix nucleate relatively later and are, thus, smaller compared to the particles on dislocations. They dissolve preferentially and the vast majority of the residual particles situate on dislocations in an overaged alloy. In coarsening stage, the N and $\langle R \rangle$ of the precipitates are not affected by the predeformations (see **Fig. 2**). These results are good in agreement with the experimental ones reported by Zhang *et al.* [**3**], indicating that the model proposed describes the precipitation of Cu particles during aging a Fe-Cu alloy well.

The effects of heating rate of the specimen, the annihilation of dislocations during the aging treatment and the dislocation density were calculated and the results are shown in **Fig. 2** and **Fig. 3**. One can conclude that the heating rate shows a weak effect on the peak position of N as well as its corresponding $\langle R \rangle$, although it has a great effect on the microstructure evolution during the nucleation stage of Cu particles. The dislocation effect is almost independent of the annihilation of dislocations. An increasement in the dislocation density even by 5 times does not change the dislocation effect, although it causes an increase in I^{dis}.

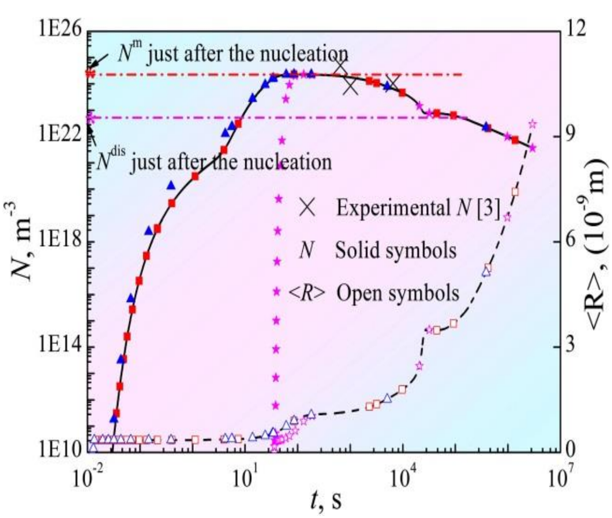

Fig. 2. Time dependence of number density (solid line) and average radius (dashed line) calculated by assuming that the initial dislocation density is 8.8×10^{13} m^{-2} and the heating rate from 298 to 773 K is 10^{6} K/s. The results calculated by neglecting the annihilation of dislocations (squares), by neglecting the dislocation effect (circles), by assuming a higher constant dislocation density of $5{\times}8.8{\times}10^{13}$ m^{-2} (triangles) and by assuming a heating rate of 10 K/s from 298 to 773 K (stars) are also shown in the figure.

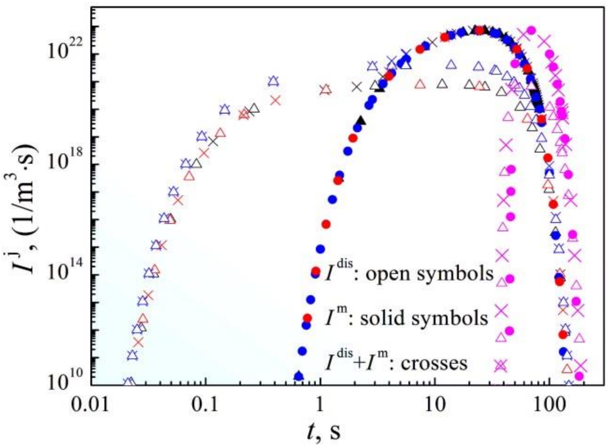

Fig. 3. Time dependence of the nucleation rates of Cu particles in the matrix (circles), on dislocations (triangles) and their sum (crosses). Black symbols are the rusults calculated by assuming that the initial dislocation density is 8.8×10^{13} m^{-2} and the heating rate from 298 to 773 K is 10^{6} K/s (as given in Fig.1). The red, blue and purple symbols respectively represent the results calculated by neglecting the annihilation of dislocations, by assuming a higher constant dislocation density of $5 \times 8.8 \times 10^{13}$ m^{-2} and by assuming a heating rate of 10 K/s from 298 to 773 K .

Conclusion

Cu particles first nucleate on dislocations and then in the matrix. But the summit of the nucleation rate in the matrix is much greater than that on dislocations and it almost remains unchanged whether the dislocations appear or not. Most of the particles situate in the matrix immediately after the nucleation. The preferential dissolution of Cu precipitates in the matrix occurs during the coarsening stage and the vast majority of the residual particles situate on dislocations in later stage of aging. Dislocations do not affect the final dispersion of particles, although they have a great effect on the nucleation behavior of the particles. The heating rate of the specimen, the dislocation density and the annihilation of dislocations during aging do not strengthen or weaken the dislocation effect.

Acknowledgements

This work was supported by the National Natural Science Foundation of China (Nos. 51771210, 51574216, 51501207), China's Manned Space Station Project (No. TGJZ800-2-RW024) and Chinese Academy of Sciences Strategic Priority Program on Space Science (No. XDA15013800).

References

1. Hornbogen, E., *Acta Metall*. **1962**, *10,* 525.
   DOI: 10.1016/0001-6160(62)90197-9
2. Deschamps, A.; Militzer, M.; Poole, W.J., *ISIJ Int.* **2001**, *41,* 196.
   DOI: 10.2355/isijinternational.41.196
3. Zhang, C.; Enomoto, M.; Yamashita, T.; Sano, N., *Metall. Mater. Trans. A* **2004**, *35,* 1263.
   DOI: 10.1007/s11661-004-0300-8
4. Yang, J.B.; Enomoto, M., *ISIJ Int.* **2005**, *45,* 1335.
   DOI: 10.2355/isijinternational.45.1335
5. Othen, P.J.; Jenkins, M.L.; Smith, G.W.D., *Philos. Mag. A* **1994**, *70,* 1.
   DOI: 10.1080/01418619408242533

6. Chen, Q.; Jin, Z.P., *Metall. Mater. Trans. A*, **1995**, *26*, 417. **DOI:** 10.1007/BF02664678
7. Mathon, M.H.; Barbu, A.; Dunstetter, F.; Maury, F.; Lorenzelli, N.; Novion, C.H., *J. Nucl. Mater*. **1997**, *245*, 224. **DOI:** 10.1016/S0022-3115(97)00010-X
8. Cahn, J.W.; Hilliard, J.E., *J. Chem. Phys*. **1958**, *28*, 258. **DOI:** 10.1063/1.1744102
9. Larche, F.C., *Solid State Phenomena*, **1994**, *35*, 173.
10. Enomoto, M. (2nd eds.); Phase Transformation in Metals; Uchida-Rokakuho: Tokyo, **2005**.
11. Salje, G.; Feller-Kniepmeier, M., *J. Appl. Phys*. **1977**, *48*, 1833. **DOI:** 10.1063/1.323934
12. Christien, F.; Barbu, A., *J. Nucl. Mater*. **2004**, *324*, 90. **DOI:** 10.1016/j.jnucmat.2003.08.035
13. Sutton, A.P.; Balluffi, R.W., Interfaces in Crystalline Materials; Clarendon Press: Oxford, **1995**.
14. Peterson, N.L., Grain-Boundary Structure and Kinetics; ASM: Metals Park, OH, **1980**.
15. He, J.; Zhao, J.Z.; Ratke, L., *Acta Mater*. **2006**, *54*, 1749. **DOI:** 10.1016/j.actamat.2005.12.023
16. Othen, P.J.; Jenkins, M.L.; Smith, G.W.D.; Phythian, W.J., *Philos. Mag. Lett*. **1991**, *64*, 383. **DOI:** 10.1080/09500839108215121
17. Zhao, J.Z.; Ratke, L.; Feuerbacher, B., *Modell. Simul. Mater. Sci. Eng*. **1998**, *6*, 123. **DOI:** 10.1088/0965-0393/6/2/003
18. Guo, J.J.; Liu, Y.; Jia, J.; Su, Y.Q.; Ding, H.S.; Zhao, J.Z.; Xue, Q., *Scripta Mater*. **2001**, *45*, 1197.

